LA-UR- 09-00077

Approved for public release; distribution is unlimited.

Title: New Insights on Geomagnetic Storms from Observations and Modeling

Author(s): V. K. Jordanova, LANL, ISR-1

Intended for: Proceedings of the School and Workshop on Space Plasma Physics,
Sozopol, Bulgaria, 1-7 September 2008

Los Alamos
NATIONAL LABORATORY
EST.1943

New Insights on Geomagnetic Storms from Observations and Modeling

Vania K. Jordanova

Los Alamos National Laboratory, Los Alamos, NM 87545, USA

Abstract. Understanding the response at Earth of the Sun's varying energy output and forecasting geomagnetic activity is of central interest to space science, since intense geomagnetic storms may cause severe damages on technological systems and affect communications. Episodes of southward (B_z<0) interplanetary magnetic field (IMF) which lead to disturbed geomagnetic conditions are associated either with coronal mass ejections (CMEs) and possess long and continuous negative IMF B_z excursions, or with high speed solar wind streams (HSS) whose geoeffectiveness is due to IMF B_z profiles fluctuating about zero with various amplitudes and duration. We show examples of ring current simulations during two geomagnetic storms representative of each interplanetary condition with our kinetic ring current-atmosphere interactions model (RAM), and investigate the mechanisms responsible for trapping particles and for causing their loss. We find that periods of increased magnetospheric convection coinciding with enhancements of plasma sheet density are needed for strong ring current buildup. During the HSS-driven storm the convection potential is highly variable and causes small sporadic injections into the ring current. The long period of enhanced convection during the CME-driven storm causes a continuous ring current injection penetrating to lower *L* shells and stronger ring current buildup.

Keywords: ring current, electric fields, plasma motion, inner magnetosphere, magnetic storms
PACS: 94.05.Sd, 94.30.cb, 94.30.cs, 94.30.Lr, 94.30.Kq, 94.30.Xy

INTRODUCTION

Geomagnetic storms are some of the most important space weather phenomena. They occur when an increase in the population of energetic ring current particles drifting around the Earth leads to an observable depression of the horizontal component of the terrestrial magnetic field, characterized by the *Dst* index. The immediate cause of magnetic storms at Earth is related to periods of southward (B_z<0) interplanetary magnetic field (IMF) reconnecting with the terrestrial magnetic field at the low-latitude dayside magnetopause [1] and allowing transfer of solar wind energy into the magnetosphere. A large fraction of this energy is stored in the storm time ring current as it builds up during the main phase of the storm. This energy is subsequently released during the recovery phase of the storm causing plasmaspheric electron and ion heating, energetic neutral and ion precipitation, and stable auroral red arcs excitation [2].

Geomagnetic storms have their origin in the structure and dynamics of the solar atmosphere. Two categories of magnetic storms have been identified based upon their solar origin; recurrent, that repeat with the solar rotation period of 27 days, or transient, that occur only once. The recurrent storms are associated with corotating interaction regions (CIRs) [3] that are formed between the high-speed streams (HSS) from coronal holes and the upstream dense slow-speed solar wind plasma [4]. The single non-recurrent events are usually associated with huge eruptions from the Sun of plasma and magnetic flux called coronal mass ejections (CMEs) and often give rise to the largest geomagnetic storms at Earth [5]. Currents induced in the ionosphere and Earth's surface during large geomagnetic storms disturb and even damage telecommunication and navigation satellites, telecommunication cables, and power grids. The aims of space weather research are thus to enhance our knowledge about the Sun and the solar wind, the magnetosphere and atmosphere, and to be able to predict adverse conditions in the space environment.

STORM MAIN PHASE

One of the main mechanisms for rapid inward transport and energization of plasma sheet particles into the ring current during the storm main phase is the development of a strong convection electric field lasting for several hours (e.g., [6]). Such a large-scale convection electric field extending from dawn to dusk across the nightside magnetosphere leads to the sunward motion of magnetospheric plasma injected far downstream in the magnetic tail. Plasmasheet particles are transported due to this **ExB** drift into regions of stronger magnetic field and are energized. To obtain the full plasma motion, one must add yet the corotation electric field caused by the Earth's rotation, important for plasma residing close to the Earth. In addition to the electric drifts of charged particles are drifts resulting from the gradient of the magnetic field strength and the curvature of the magnetic field lines. In contrast with the electric drifts, magnetic drifts are energy dependent, therefore they are negligible for low energies ~1 eV (thermal plasma) and they are dominant for high energies ~1 MeV (radiation belt particles). For ring current particles at intermediate energies (~1-200 keV), both the electric and magnetic drifts have comparable importance in the determination of the particle trajectories. Furthermore, since the gradient-curvature drift is charge dependent, ions drift westward around the Earth, while electrons drift eastward and a current is formed around the Earth called the ring current. Finally, we should note that over long periods of time high energy particles can diffuse radially as a result of resonant interactions with the fluctuating components of the convection [7]. This interaction is described as radial diffusion because it results in transport of particles across the dipolar-like magnetic field lines in radial direction.

To study the stormtime transport and acceleration of energetic particles, a kinetic ring current – atmosphere interactions model (RAM) was developed by Jordanova et al. [8, 9]. The phase space distribution function in RAM is defined for variables that are accessible to direct measurement, i.e., energy, pitch angle, radial distance in the equatorial plane and magnetic local time (MLT). The model thus solves the bounce-averaged kinetic equation for H^+, O^+, and He^+ ions with kinetic energy from ~100 eV to 400 keV and pitch angle from 0° to 90°. A region in the equatorial plane spanning radial distances from 2 R_E to 6.5 R_E and all magnetic local times (MLT) is included. The inflow of plasma from the magnetotail is modeled according to the total ion flux measurements from the Magnetospheric Plasma Analyzer (MPA) and the Synchronous Orbit Particle Analyzer (SOPA) instruments on the geosynchronous Los Alamos National Laboratory (LANL) satellites and the ion composition ratios are inferred from the work of Young et al. [10]. In recent work Jordanova et al. [11] used this model to address the processes of ring current formation during the 22-23 April 2001 and 24-26 October 2002 storms of similar strength (*Dst* index reaching minimum values of about -100 nT) but different solar origin. The interplanetary observations during 22-23 April 2001 from the instruments on ACE spacecraft indicated a relatively smooth south-to-north B_z excursion of the IMF characteristic of a CME, leading to a gradually increasing interplanetary electric field (IEF) and monotonically decreasing *Dst*. In contrast, the interplanetary medium on 24 October 2002 showed a stream-stream interaction (a HSS overtaking a slower stream) during which the southward B_z component of the IMF was highly fluctuating, leading to high temporal variations of the IEF and a step-like decreasing *Dst*.

We simulated ring current development during these two large geomagnetic storms and investigated the effect of magnetospheric convection with our RAM using three different electric field formulations. In Figure 1 we compare results from (1) a *Kp*-dependent Volland-Stern (V-S) electric potential model [12, 13, 14]; (2) a Volland-Stern model including a potential drop from subauroral polarization streams (SAPS) [15], and (3) the UNH-IMEF model [16, 17] driven by interplanetary conditions. The analytical V-S model predicts the largest electric potential during the main phase of the storms when maximum *Kp* is observed, at hours ~39 to 41 during both storms (Figure 1, top). Including SAPS disturbance effects makes this model stronger and more realistic, creating a day-night asymmetry and skewing the potential in the postmidnight sector as seen in self-consistent electric field model simulations [e.g., 18]. The UNH-IMEF model is derived from electric field data primarily from the Cluster satellites. This electric field data set is sorted according to several ranges of the IEF values measured by ACE and includes statistical results from ground radars and low altitude satellites inside the perigee of Cluster (4 R_E). Its magnitude increases for larger IEF values, which occur during the main phase of the storms when IMF B_z maximizes, at hour ~34 during the April 2001 storm (Figure 1a) and at hour ~36 during the October 2002 storm (Figure 1e). The plasma sheet ion density from the MPA (Figures 1b and 1f) are plotted along the nightside orbit of the LANL satellites (between MLT=18 and MLT=6) and exhibit temporal as well as spatial variations. The data indicate that the ring current source population is highly variable throughout the intervals. Enhanced density is observed during the main phase of both storms with peak values from ~1.5 to 2 cm^{-3} during April 2001 and from ~1 to 1.5 cm^{-3} during October 2002. The ring current injection rate calculated with RAM and defined as the total energy gain per hour (Figures 1c and 1g) reflects the variations of the convection potential and the inflow of plasma at the nightside boundary. There is primarily one long-term enhancement on 22 April (Figure 1c) during the main phase of the CME-driven storm. This enhancement peaks at hour ~34.5 using UNH-IMEF model, and at hour ~40.5 using V-S or VS-SAPS models. In contrast, several short-term intensifications occur during 24 October (Figure 1g) corresponding to the increase of the convection strength and plasma sheet density during the main phase of this HSS-driven storm. The convection potential predicted with UNH-IMEF model is smaller and leads to a smaller injection rate than using VS or VS-SAPS model during both storms.

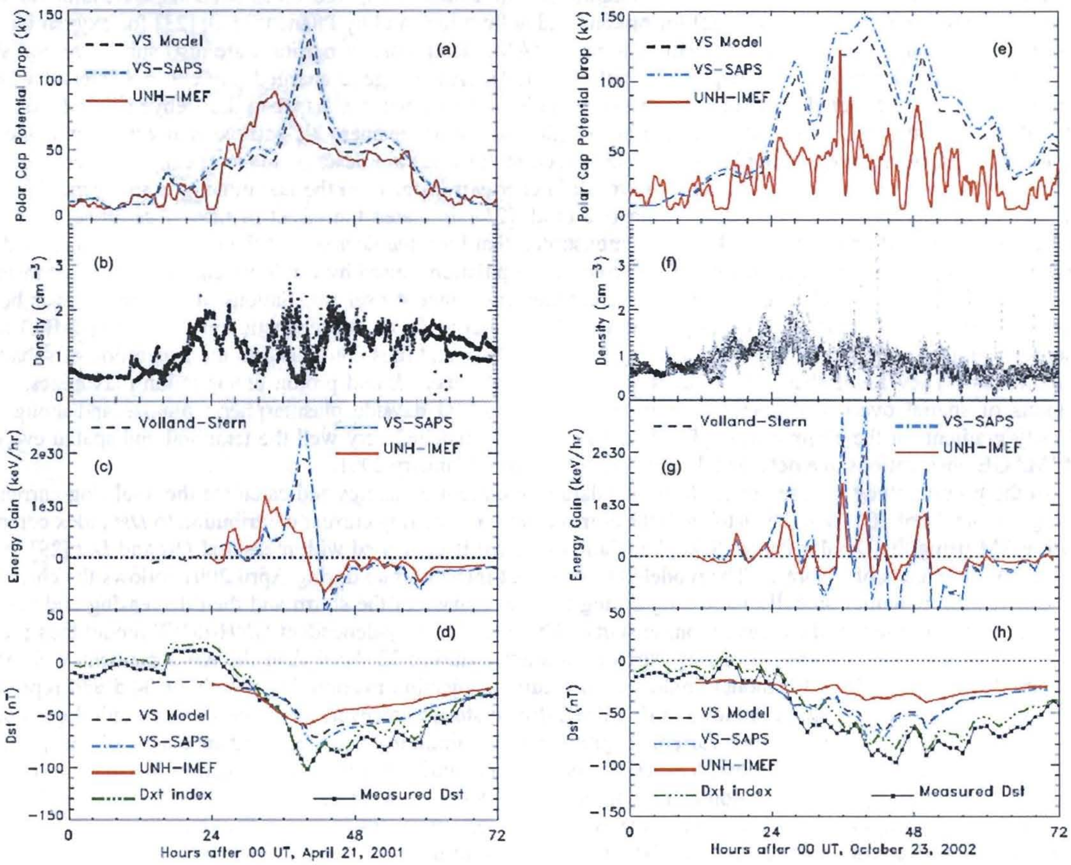

FIGURE 1. (a, e) Polar cap potential drop obtained with the Volland-Stern model (dashed line), Volland-Stern model including SAPS (dash-dotted blue line), and the UNH-IMEF model (solid red line). (b, f) Nightside plasma sheet ion density at geosynchronous orbit. (c, g) Calculated ring current injection rate using V-S model (dashed), VS-SAPS model (dash-dotted), and UNH-IMEF model (solid). (d, h) Computed *Dst* index using the three model formulations compared with measured *Dst* (starred line) and *Dxt* (dash-dot-dotted green line) indices. The left panels (a), (b), (c), and (d) refer to the April 2001 storm, while the right panels (e), (f), (g), and (h) refer to the October 2002 storm.

STORM RECOVERY PHASE

The ring current decay during the recovery phase of the magnetic storm leads to the restoration of the surface magnetic field of the Earth to its pre-storm values. Ring current particles are lost due to collisions with neutral atoms from the upper atmosphere as well as with low-energy plasmaspheric particles, and are subject to interactions with plasma waves. In addition, particles are lost at the dayside magnetopause when they flow out of the trapping region [e.g., 19]. Ring current energy is deposited into the thermosphere-plasmasphere system through particle and heat fluxes causing heating of the neutral atmosphere and the plasmasphere, ionization, subauroral emissions, and other aeronomical effects.

All major ring current loss processes are included in our global physics-based RAM. A very important loss mechanism for ring current ions is charge exchange with neutral hydrogen from the geocorona. The probability of collisions with neutral atoms from the exosphere depends on the energy of the incident particles and is determined by the charge exchange cross sections. Proton charge exchange cross sections over most of the radiation belt energy range have been compiled from measurements and theoretical studies by Spjeldvik [20], and those including heavier ions by Smith and Bewtra [21]. Recent compilations of charge exchange cross sections, extending to lower energies, were provided by Barnett [22] for protons and helium ions and by Phaneuf et al. [23] for oxygen ions and these are the charge exchange cross sections used in RAM. Ring current particles are also subject to collisional interactions with coexisting plasmaspheric populations [24]. An energetic charged particle will interact with the electric field of a thermal electron or ion, whenever the impact parameter is less than the Debye shielding distance. Despite the fact that these encounters are not binary (the motion of the energetic particle is affected simultaneously by the field of many background plasma particles), such interactions are described theoretically as a series of weak binary collisions. These binary collisions will result in energy transfer from the fast moving to the thermal ion, and in angular deflection of both particles. Jordanova et al. [25] simulated the effect of these loss processes on ring current ions with arbitrary pitch angles and demonstrated that both the decrease of the distribution function due to charge exchange losses and the buildup of a low-energy population caused by Coulomb collisions proceed faster for particles with smaller pitch angles, since such particles encounter denser populations along their longer bounce paths. Recently, Jordanova et al. [26] demonstrated that scattering by electromagnetic ion cyclotron (EMIC) waves increases significantly the ion precipitation into the atmosphere and thus could lead to the generation of subauroral proton arcs. They found that EMIC waves are preferentially excited, and proton precipitation maximizes, within regions of spatial overlap of energetic ring current protons and dayside plasmaspheric plumes and along steep density gradients at the plasmapause. The RAM simulations matched very well the temporal and spatial evolution of IMAGE observations of a detached dayside proton arc on 23 January 2001.

In the present study we use our RAM to simulate ring current dynamics and calculate the total ring current ion energy as the April 2001 and the October 2002 storms develop. The ring current contribution to *Dst* index computed with RAM using the Dessler-Parker-Sckopke relation [27, 28] is compared with measured *Dst* and *Dxt* [29] indices in the bottom panels of Figure 1. The modeled ring current injection rate during April 2001 follows the changes of the convection potential, initially increasing during the main phase of the storm and then decreasing and reaching minimum at the time that the recovery phase starts. The interplanetary-dependent UNH-IMEF model thus predicts quite different temporal variation of ring current parameters during 22 April than the *Kp*-dependent V-S models (Figure 1d). The UNH-IMEF model predicts a ring current injection maximizing near hour 34.5 and reproduces very well the initial ring current buildup of this CME-driven storm; however, its convection strength drops quickly and the model underestimates ring current magnitude near minimum *Dst*. The enhancement of the polar cap potential drop predicted with V-S and VS-SAPS models peaks during the period of enhanced plasma sheet density and causes large ring current injection and minimum *Dst* ~ -80 nT at hour 42, a few hours after measured *Dst* and *Dxt* minima. During October 2002 (Figure 1h) every ion injection causes an intensification of the ring current and subsequently a decrease in the calculated *Dst*. The ring current decays when the loss processes dominate and the injection rate becomes negative. All models thus predict several dips in the simulated *Dst* that match very well the drops in measured *Dst* and *Dxt*. However, the UNH-IMEF model predicts small intermittent enhancements which are not sufficient to build a strong ring current during this HSS-driven storm. The enhancements predicted with VS-SAPS model are the largest and this model reproduces best the measured *Dst* index (but still overestimates its minimum with ~25 nT, the agreement with the *Dxt* index is better). We find that while RAM simulations using any magnetospheric electric field model reproduced the main trends of ring current formation and decay, they all more or less underpredicted the *Dst* values at storm peak. Additional injections from radial diffusion due to magnetic field fluctuations usually improve the agreement with *Dst* during the storm recovery phase [30, 31]. Contributions from substorm injections [32], magnetotail currents [33], and ring current electrons [34] could also bring better agreement with *Dst* and *Dxt* indices.

CONCLUSIONS

A brief summary of recent observations and modeling efforts regarding geomagnetic storm dynamics and ring current formation and decay is presented in this paper. With the increase of available multi-satellite data and computer capabilities, numerical models have become more realistic. Most of the models thus include nonequatorially mirroring ions, allowing the investigation of the latitudinal distribution of the ring current. We show simulations of ring current evolution during two geomagnetic storms of different solar origin, a CME-driven storm and a HSS-driven storm. The models are able to reproduce the stormtime ring current flux enhancements caused by an increased convection electric field, showing qualitative agreement with observations. However, good quantitative agreement has been difficult to obtain, probably due to the use of simplified electric and magnetic field models. In order to address the effect of induced electric fields on ring current formation, a full theoretical model of ring current injection with self-consistently computed electric and magnetic fields is necessary to be developed.

Ring current particle populations are also affected by source and loss mechanisms. The plasma sheet ion population has been recognized as the predominant source for the ring current. A remaining problem to be resolved though is the relative contribution of ionospheric and solar wind sources to ring current formation. Ring current losses due to both charge exchange and Coulomb collisions are sufficiently well understood, and the predominant role of charge exchange in ring current decay has been established. Losses due to wave-particle interactions are, however, not easy to treat theoretically on a global scale, mostly because of the difficulty of estimating the wave spectrum, and their effect on ring current and radiation belt dynamics requires further investigation. Finally, we should note that most of the studies at present consider the dynamics of ring current ions; the electron component of the ring current has to be investigated in detail in future work.

ACKNOWLEDGMENTS

This work was conducted under the auspices of the U. S. Department of Energy, with partial support from the NASA Theory, LWS, and GI programs, and from a Los Alamos National Laboratory Directed Research and Development grant.

REFERENCES

1. J. W. Dungey, *Phys. Res. Lett. 6*, 47 (1961).
2. M. H. Rees and R. G. Roble, *J. Geophys. Res.* **13**, 201 (1975).
3. E. J. Smith and J. H. Wolf, *Geophys. Res. Lett.* **3**, 137 (1976).
4. N. U. Crooker and E. W. Cliver, *J. Geophys. Res.* **99**, 23383, (1994).
5. B. T. Tsurutani, W. D. Gonzalez, F. Tang and Y. T. Lee, *Geophys. Res. Lett.* **19**, 73 (1992).
6. W. D. Gonzalez, J. A. Joselyn, Y. Kamide, H. W. Kroehl, G. Rostoker, B. T. Tsurutani and V. M. Vasyliunas, *J. Geophys. Res.* **99**, 5771 (1994).
7. C.-G. Fälthammar, *J. Geophys. Res.* **70**, 2503 (1965).
8. V. K. Jordanova, J. U. Kozyra, G. V. Khazanov, A. F. Nagy, C. E. Rasmussen and M.-C. Fok, *Geophys. Res. Lett.* **21**, 2785 (1994).
9. V. K. Jordanova, "Kinetic model of the terrestrial ring current", Ph.D. Thesis, Univ. of Michigan, Ann Arbor, 1995.
10. D. T. Young, H. Balsiger and J. Geiss, *J. Geophys. Res.* **87**, 9077 (1982).
11. V. K. Jordanova, H. Matsui, P. A. Puhl-Quinn, M. F. Thomsen, K. Mursula and L. Holappa, *J. Atm. Sol. Terr. Phys.* doi:10.1016/j.jastp.2008.09.043 (2009).
12. H. Volland, *J. Geophys. Res.* **78**, 171 (1973).
13. D. P. Stern, *J. Geophys. Res.* **80**, 595 (1975).
14. N. C. Maynard and A. J. Chen, *J. Geophys. Res.* **80**, 1009 (1975).
15. J. Goldstein, J. L. Burch and B. R. Sandel, *J. Geophys. Res.* **110**, A09222, doi:10.1029/2005JA011135, (2005).
16. H. Matsui, V. K. Jordanova, J. M. Quinn, R. B. Torbert and G. Paschmann, *J. Geophys. Res.* **109**, A10202, doi:10.1029/2003JA010319 (2004).
17. P. A. Puhl-Quinn, H. Matsui, V. K. Jordanova, Y. Khotyaintsev and P.-A. Lindqvist, *J. Atm. Sol.-Terr. Phys.* doi:10.1016/j.jastp.2007.08.069 (2008).
18. R. A. Wolf, "The quasi-static (slow-flow) region of the magnetosphere", in *Solar-Terrestrial Physics*, edited by R. L. Carovillano and J. M. Forbes, D. Reidel, Norwell, Mass., 1983, pp. 303-368.
19. S. Takahashi, T. Iyemori and M. Takeda, *Planet. Space Sci.* **38**, 1133 (1990).
20. W. N. Spjeldvik, *J. Geophys. Res.* **82**, 2801 (1977).
21. P. H. Smith and N. K. Bewtra, *Space Sci. Rev.* **22**, 301 (1978).
22. C. F. Barnett, Tech. Rep. ORNL-6086/VI, Oak Ridge, Tenn., 1990.
23. R. A. Phaneuf, R. K. Janev and M. S. Pindzola, Tech. Rep. ORNL-6090/V5, Oak Ridge Nat. Lab., Oak Ridge, Tenn., 1987.
24. R. C. Wentworth, W. M. MacDonald and S. F. Singer, *Phys. Fluids* **2**, 499 (1959).

25. V. K. Jordanova, L. M. Kistler, J. U. Kozyra, G. V. Khazanov and A. F. Nagy, *J. Geophys. Res.* **101**, 111 (1996).
26. V. K. Jordanova, M. Spasojevic and M. F. Thomsen, *J. Geophys. Res.* **112**, A08209, doi:10.1029/2006JA012215 (2007).
27. A. J. Dessler and E. N. Parker, *J. Geophys. Res.* **64**, 2239 (1959).
28. N. Sckopke, *J. Geophys. Res.* **71**, 3125 (1966).
29. A. Karinen and K. Mursula, *Ann. Geophys.* **23**, 475 (2005).
30. V. K. Jordanova, Y. S. Miyoshi, S. Zaharia, M. F. Thomsen, G. D. Reeves, D. S. Evans, C. G. Mouikis and J. F. Fennell, *J. Geophys. Res.* **111**, A11S10, doi:10.1029/2006JA011644 (2006).
31. V. K. Jordanova, "Modeling the behavior of corotating interaction region driven storms in comparison with coronal mass ejection driven storms", in *Recurrent Magnetic Storms: Corotating Solar Wind Streams*, Geophys. Monogr. Ser., vol. 167, edited by B. T. Tsurutani et al., AGU, Washington, D. C., 2006, p. 77.
32. N. Y. Ganushkina et al., *J. Geophys. Res.* **105**, 25205 (2000).
33. N. E. Turner, D. N. Baker, T. I. Pulkkinen and R. L. McPherron, *J. Geophys. Res.* **105**, 5431 (2000).
34. V. K. Jordanova and Y. Miyoshi, *Geophys. Res. Lett.* **32**, L14104, doi:10.1029/2005GL023020 (2005).